To appear in SPIE Proceedings Vol. 3403 (February 1998).

Environmental monitoring of chemical species

Frank K. Tittel and K.P. Petrov
Rice Quantum Institute, Rice University
P.O. Box 1892, Houston, Texas 77251-1892

ABSTRACT

Design, development, and application of novel all-solid-state spectroscopic gas sensors is reported. These compact instruments employ mid-infrared difference-frequency generation in a nonlinear optical medium pumped by room-temperature semiconductor lasers, and are capable of real-time selective measurement of trace gases in ambient air with better than 1 ppb precision (part per billion, by mole fraction).

1. INTRODUCTION

In recent years there has been an increasing interest in *field* detection and precise measurement of environmentally important atmospheric trace gases such as nitric oxide (NO), carbon monoxide (CO), nitrous oxide (N_2O), formaldehyde (H_2CO), methane (CH_4), and surfur dioxide (SO_2). Applications that require such measurements include air quality control; atmospheric chemistry; mapping of agricultural, landfill, and traffic emission; and pipeline leak detection. In addition to gas concentration, applications such as landfill emissions monitoring require measurements of gas fluxes and isotopic ratios.

There are several competing technologies in mid-infrared atmospheric sensing. FTIR and lead-salt diode laser systems which are semi-portable are currently being utilized in the field. (A semi-portable sensor can be moved from location to location by truck and set up reasonably conveniently in the new location. Our sensor is portable but is not yet *rugged* enough for portable field operations. It has been operated in the field as a semi-portable device.) As compared with readily portable FTIR sensors which typically have a resolution of 1 cm^{-1} or greater, DFG offers individual pressure broadened (or even Doppler broadened) line resolution.[1,2] Room temperature operation provides a significant advantage to diode-pumped DFG, as compared with lead-salt diode lasers,[3,4] which require cryogenic cooling for normal operation. A promising, but as yet unrealized for sensing applications, development of electrically and optically pumped III-V semiconductor lasers at 2.0-4.5 μm has been reported.[5,6] To date, these lasers still require cooling to ~100 K for continuous-wave operation, but eventually operation at temporatures above 200 K is expected, at which time they may become useful for IR monitoring. Operation of CW quasi-phase-matched optical parametric oscillators (OPO) has also been reported.[7,8] Diode-pumped CW OPO's may become attractive sources for use in high-resolution spectroscopy and trace gas detection, but further development is needed to alleviate their present shortcomings. These include unreliable single-frequency operation and lack of predictable fast wavelength control.

In this report we describe the development and application of a portable all-solid-state gas sensor based on diode-pumped mid-infrared DFG, capable of achieving detection limits of better than 10 ppb for several important trace gases in air at atmospheric pressure. Earlier feasibility tests[9] have indicated that this can be done with the use of periodically poled lithium niobate (PPLN), a novel infrared nonlinear material that is now commercially available. Its quasi-phase-matching properties can be tailored for DFG in the 2-5 μm region with many commercial diode and diode-pumped solid-state lasers. This, along with large nonlinearity and good optical quality, makes PPLN the ideal mixing material for DFG applications targeted at species like CO, N_2O, CO_2, SO_2, H_2CO, and CH_4.[10,11]

2. INSTRUMENT DESCRIPTION

A diagram of the optical section of the gas sensor is shown in Figure 1. Our choice of the laser pump sources was motivated primarily by their capability of reliable single-frequency, low-noise operation over extended periods of time in an environment where vibration and changes in temperature and humidity are commonplace.[12] The signal source is a diode-pumped non-planar monolithic ring Nd:YAG laser with 750 mW output power at 1064.5 nm (Lightwave Electronics, Inc., Model 126). The pump source is a 100 mW solitary GaAlAs diode laser at 865 nm (SDL, Inc., Model 5412), hermetically sealed in a TO-3 metal package together with a thermoelectric cooler, a monitor photodiode, and a thermistor. The laser is attached to a stable mirror mount, and its output is collimated by an F = 8 mm multi-element lens with 8 mm aperture.

The lens is held by two eccentric rings mounted in the adjustable front plate of the mirror mount. Such an arrangement provided precise, long-term stable alignment of the lens in three dimensions with minimum sensitivity to vibration.

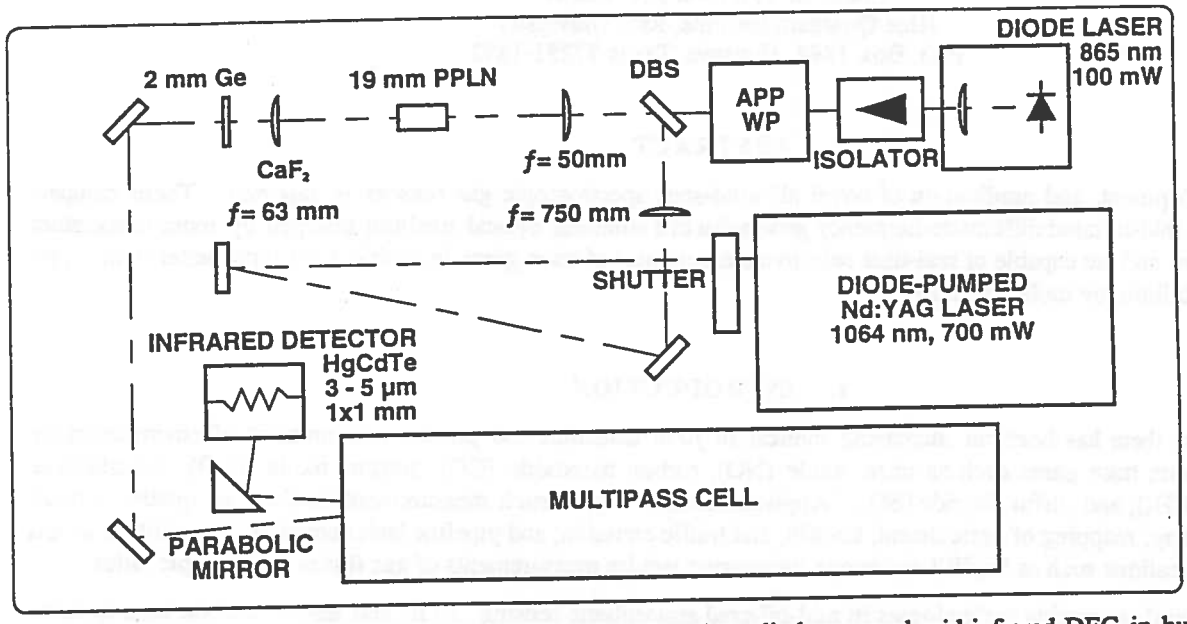

Figure 1: Schematic of a portable sensor for trace gas detection, based on diode-pumped mid-infrared DFG in bulk PPLN. APP – anamorphic prism pair, WP – half-wave plate, DFB – dichroic beamsplitter.

The output of the diode laser passes through a compact 40 dB isolator with an 8 mm × 2 mm rectangular aperture (Electro-Optics Technology, Inc., Model 1845), a half-wave plate, and a 4× anamorphic prism pair, emerging as a vertically polarized beam 1.9 mm in diameter and nearly mode-matched to the signal beam for efficient DFG. The pump and signal beams are combined by a dichroic beamsplitter and focused into an uncoated PPLN crystal measuring 19 mm × 11 mm × 0.5 mm (Crystal Technology, Inc.). The z-cut crystal has eight 1.5 mm wide stripes with domain grating periods ranging from 22.4 μm to 23.1 μm in 0.1 μm steps. For difference-frequency mixing at 4.6 μm (idler), the optimum period was found to be 22.9 μm at room temperature.

The pump and signal beams enter the PPLN crystal at near normal incidence to the domain grating. With 70 mW pump power at 865 nm and 750 mW signal power at 1064.5 nm incident on the crystal, a typical idler power of 4.4 μW was measured. This value is in good agreement with 5 μW calculated from the theory of Chu and Broyer.[13] The calculation accounts for Fresnel losses at the facets of the crystal and significant absorption losses in lithium niobate at 4.6 μm. Measurements by Myers[14] suggest transmission of only 25% for the extraordinary beam in a 19 mm long PPLN crystal at this wavelength. A 12% discrepancy between the measured and calculated power is due to the onset of beam clipping at the output of the crystal. The idler beam is collimated with an F = 63 mm uncoated calcium fluoride lens and separated from the pump and signal beams by a germanium filter.

The idler beam is than directed into a compact multipass cell (New Focus, Inc., Model 5611) aligned for an effective path length of 18.3 m. The cell was used to increase the measured optical absorption by CO in air to at least 1%, so that the measured signal may substantially exceed detector noise and optical interference. Absorption signals of this magnitude could be easily observed in the presence of linear amplitude modulation associated with frequency tuning of the pump laser. The path length of 18 m is achieved with 93 passes between mirrors separated by 20 cm. Optical throughput of the cell was measured to be 38%. An F = 35 mm off-axis parabolic mirror collected the idler beam at the output of the cell.

Measurements of idler power were initially performed with the use of a liquid-nitrogen-cooled photovoltaic InSb detector. The results were used to calibrate the response of a HgCdTe detector with 1 mm^2 active area (EG&G Judson, Inc., Model J15TE3:5), cooled to -65°C by a three-stage Peltier cooler. The detector is biased at 1.2 mA and dc-coupled to a low-noise preamplifier with a voltage gain of 350 and gain bandwidth of 200 kHz. The detector/preamplifier system has a response of 0.46 $V \cdot \mu W^{-1}$ and a noise-equivalent power of 3.3 $pW \cdot Hz^{-1/2}$ at 4.6 μm, with a typical output voltage drift of 0.25 $mV \cdot hr^{-1}$ in the dark state. Low-drift dc coupling of the detector allowed the direct measurement of idler power necessary to determine percent optical absorption. Typical idler power measured after the multipass cell was 1.5 μW.

Output of the preamplifier was digitized with a 16 bit, 200 kS/s analog-to-digital converter – part of a PCMCIA data acquisition card (National Instruments, Inc., Model AI-16XE-50). The card served as an interface to a laptop computer running a LabVIEW program. Digital output of the card was used to control a small mechanical shutter to block the Nd:YAG beam for 10 s every 3 minutes, allowing the measurement of dark detector voltage. A time trace of detector voltage V(x) averaged over 10 to 1000 sweeps, with dark voltage V_{dark} subtracted, constituted a spectroscopic measurement:

$$In(V(x)-V_{dark}) = \frac{a_0}{1+\frac{(x-a_1)^2}{a_2^2}} + In(a_3 + a_4 \cdot x) \quad (1)$$

where x is the time index, a_0 is the peak absorbance, a_1 is the peak center, a_2 is the peak half-width a half-maximum, and $a_3 + a_4 \cdot x$ accounts for linear modulation of idler power associated with frequency tuning.

The equation was employed in nonlinear least-squares fitting of absorption apectra with the use of the Levenberg-Marquardt method.[15] Typical values of peak absorbance a_0 observed for the R(2) transition of CO in room air were 0.01 - 0.02; they were used to compute the CO mole fraction in parts per billion (ppb). Depending on the number of averages, the result could be updated every 1 to 20 seconds.

Direct absorption spectroscopy was chosen in this application because it offers adequate precision combined with the ease of signal provessing and calibration. Alternatively, wavelength-modulation spectroscopy[16] can be used, provided the modulation frequency falls within the gain bandwidth of the detector/preamplifier. This method is attractive because of efficient reduction of noise bandwidth. However, it requires more sophisticated signal processing and calibration techniques.

The entire optical setup, along with power supplies and electronics, is contained in a 1 ft × 1 ft × 2 ft aluminum case. The instrument draws less than 50 W electrical power and can be operated from car batteries.

3. CO CONCENTRATION MEASUREMENTS

Mid-infrared frequency scans were performed by a 58 Hz, 30 mA peak-to-peak triangular modulation of the diode laser drive current. This corresponds to a tuning range of approximately 30 Ghz, sufficient for capturing a single atmospheric pressure-broadened transition of carbon monoxide.

Nitrous oxide (N_2O) was used as a reference gas to determine the operating wavelength. Figure 2 shows a portion of the reference spectrum near 2154.5 cm^{-1} at a presure of 2.5 Pa in the multipass cell, with a correction made for the linear amplitude modulation associated with frequency tuning. The trace is a 512 sweep average. The observed transitions were identified with the help of References 11, 17, and 18 and are listed in Table 1. Peaks 7 and 9 could not be identified with the available literature. Their frequencies are given with an uncertainty equal to the maximum deviation of the experimental frequency axis from a straight line, based on the assignments by Maki and Wells.[11] Peak 5 was identified as the R(2) fundamental transition of CO. Frequency resolution of the instrument was better than 200 Mhz, inferred from the spectroscopy of the P(28) doublet of N_2O near 2169.2 cm^{-1}. We observed interference fringes in the multipass cell due to scattering, as indicated by the ×200 magnified section of Figure 2. This interference limited the signal-to-noise ratio to 300 in the averaged trace. The trace contains 1024 points which can be transformed to give 513 Fourier components. The full scale signal-to-noise ratio can be improved to better than 10,000 by application of a low-pass Gaussian filter F_k that weights the higher frequency Fourier components of the trace to zero:

$$F_k = \exp\left[-\frac{k^2}{32^2}\right], \qquad k = 0...512 \quad (2)$$

The filter works better with spectra obtained at atmospheric pressure becauseeak widthsme much larger than the period of interference. Figure 3 shows a specthe R(2) fundamental transition of CO at 2154.595582 cm^{-1} [11] in room air at atmospheric pressure. The dots represent the measured data – a 100 sweep average corrected for the linear amplitude modulation associated with frequency tuning. The thick solid trace is a fit to a Lorentzian profile. The CO mole fraction computed from the fit is 324 ± 6 ppb. The error given corresponds to the root mean squared (RMS) fit residuals, plotted with a thin solid line. The relatively high-frequency interference fringes result from scattering in the multipass cell. An absorption of water at 2154.7 cm^{-1} produces noticeably large fit residuals to the left of the CO absorption peak.

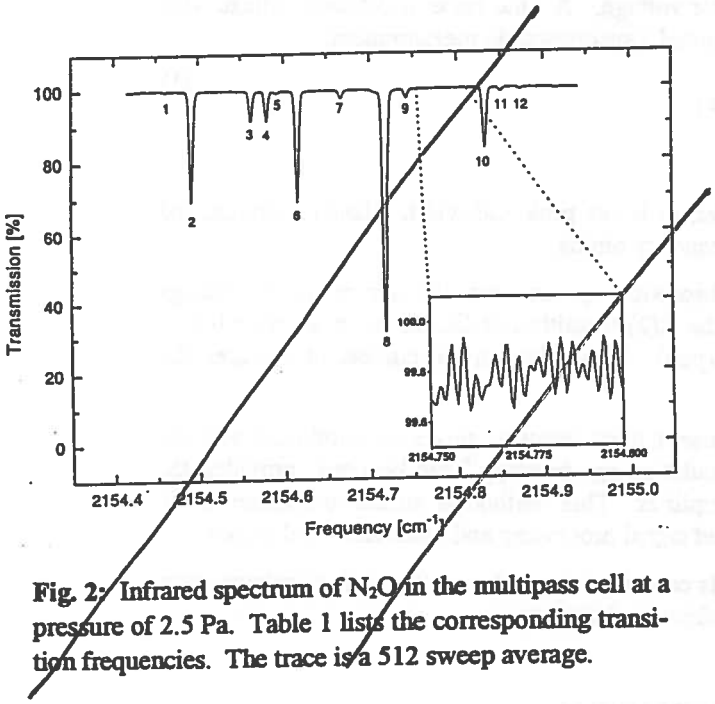

Fig. 2: Infrared spectrum of N_2O in the multipass cell at a pressure of 2.5 Pa. Table 1 lists the corresponding transition frequencies. The trace is a 512 sweep average.

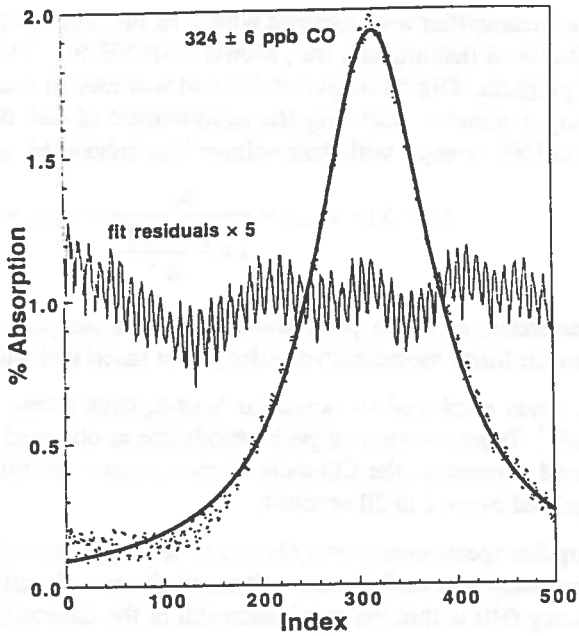

Fig. 3: A spectrum of the R(2) fundamental transition of CO in room air at atmospheric pressure. The dots represent a 100 sweep averaged signal.

For calibration of the DFG sensor, we measured absorption by CO in air flowing from a high-pressure cylinder (Scott Specialty Gases, Inc.). The factory-assigned CO mole fraction in the cylinder was 9000 ± 50 ppb. The measurements were performed at a flow rate of 300 $cm^3 \cdot min^{-1}$ at atmospheric pressure, with 2.5 s interval between data points for 100 s (Fig. 4) and yielded the absorbance $a_0 = 0.5382 \pm 0.0005$. The qualtity 0.0005 is the standard deviation of individual values of absorbance. Typical value of the RMS fit residuals in this experiment was 0.0013 absorption units, equivalent to 20 ppb CO. The primary sources of the fitting error were interference by water, and the fact that the fitting was performed to a Lorentzian rather than a Voigt profile. The value of a_0 normalized to CO mole fraction in the sample is the calibration contract: $(5.980 \pm 9.996) \cdot 10^{-5} \cdot ppb^{-1}$. The error given here does not include the uncertainty in concentration of the reference sample. Including this uncertainty implies a calibration constant of $(5.98 \pm 0.04) \cdot 10^{-5} \cdot ppb^{-1}$. This compares well with the number $(5.95 \pm 0.06) \cdot 10^{-5} \cdot ppb^{-1}$ calculated from the GEISA database,[10] assuming an optical path length of 18 ± 0.2 m.

Similar measurements were performed over the course of three weeks with two cylinders of calibrated air with factory-assigned CO mole fractions of 1030 ± 55 ppb (Figure 5) and 9000 ± 50 ppb. The measurements yielded typical standard deviations of 1 to 3 ppb for the signal averaging time of 20 s. The accuracy of these measurements was 0.6%, limited by uncertainty in the assignment of the reference sample (9000 ± 50 ppb).

Unattended operation of the instrument was recorded over extended periods of time in order to investigate the drift in alignment, output power, frequency, and spectroscopic baseline profile. Infrared output power showed a typical 20% peak-to-peak variation in the course of a day. The variation appears to be caused by thermal drift in optical alignment, since the output power level recovered at the end of each 24 hour period after initial alignment. Maximum frequency drift observed in a course of a day was ~0.5 Ghz. The drift was tracked (in the form of a_1) by the data fitting algorithm, and did not affect the mesurements of concentration.

Figure 6 shows a record of CO concentration in laboratory air over 24 hours. The multipass cell was left open in this experiment to allow convective flow of air (air temperature and pressure were not monitored). Each data point corresponds to a 512 sweep average acquired every 10 seconds. The two peaks in Figure 6 were observed during the morning and evening rush house, and appear somewhat delayed in time. We have recorded such behavior of the CO concentration on a consistent basis over six weeks. Stability of the spectroscopic baseline profile was judged by the value of the RMS fit residuals, which did not vary by more than 50%, despite the sometimes large swings in the magnitude of absorption signal (Figure 6).

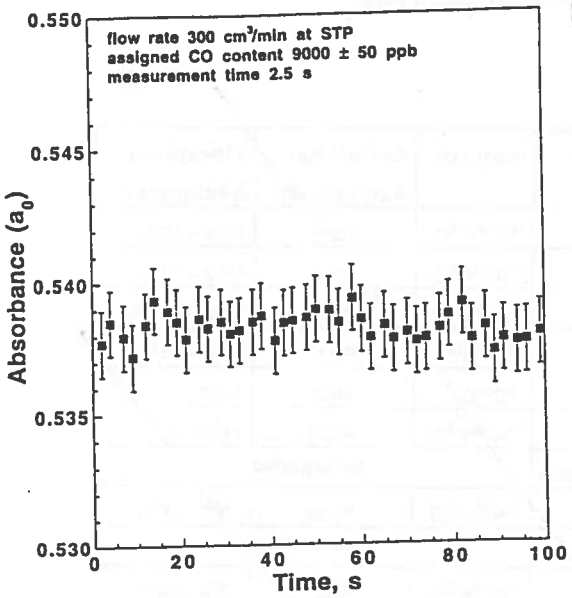

Fig. 4: CO peak absorbance (versus time in the calibration experiment. The air from a high-pressure cylinder has a factory-assigned CO content of 900 ± 50 ppb. The measured absorbance normalized to the CO concentration is (5.980 ± 0.006) × 10^{-5} · ppb^{-1}.

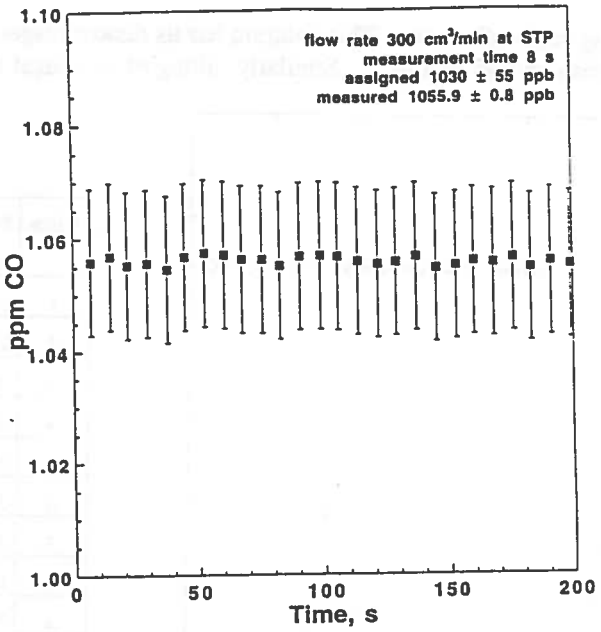

Fig. 5: Measurement of air sample with factory-assigned CO content of 1030 ± 55 ppb. The value measured in the experiment is 1055.9 ± 0.8 ppb, based on the calibration data from Fig. 4. The standard deviation of 0.8 ppb does *not* include the undertainty of calibration (~6 ppb).

The instrument can be modified for the detection of other trace gases. The simplest method is to tune the pump wavelength by temperature control to reach the desired idler wavelength. A tuning range of ~50 cm^{-1} can be achieved this way. Alternatively, an external-cavity diode laser (SDL, Inc., Model 8610 for example) can provide a tuning range of ≥700 cm^{-1} (816 nm to 865 nm).[19] Adjustment of the PPLN grating period will be required in either case and can be performed with the use of a single crystal such as the one described above.

4. REDUCTION OF INTERFERENCE AND NOISE

The optical train of the high-precision DFG sensor must satisfy the following requirements. First, it must have high overall optical transmission in order to maximize detected signal. The larger the signal, the less likely will the measurement be limited by detector noise. This requirement is met by minimizing the number of beam shaping elements and application of anti-reflection coatings where possible.

The second requirement is that the transmission must be independent of wavelength in the region where spectral scans are performed. The problem is that change in transmission with wavelength can be interpreted as stray absorption. It generally cannot be distinguished from real absorption in a single spectrum. The problem becomes critical in real-time and remote sensing applications in which baseline spectra can not be obtained. Stray absorption can be modeled and numerically eliminated if its origin is known and characteristics are predictable. The better solution, of course, is to eliminate stray absorption by design. To see how this is done, let us look at the most common cases of stray absorption.

Etalon fringes are perhaps the most common and annoying example of stray absorption. A pair of optically polished interfaces may form an etalon. The interfaces do not have to be flat or even exactly parallel to each other. They often act as a low-finesse etalon, with changes in transmission not exceeding 10%. Anti-reflection coating of the interfaces can reduce finesse by a factor of 20-500, bringing stray absorption down to a fraction of a percent, but that is still a significant error in a precision spectrometer trying to measure absorption of 1% or less. Besides, not all interfaces can be readily coated for desired wavelength, or sometimes even two wavelengths, so the more practical solution is to mount interfaces at an angle to the

beam, eliminating back-reflections. This solution has its disadvantages. For example, tilting of a lens or placing it off center introduces astigmatism and distortion. Similarly, tilting of an optical isolator lowers its return loss.

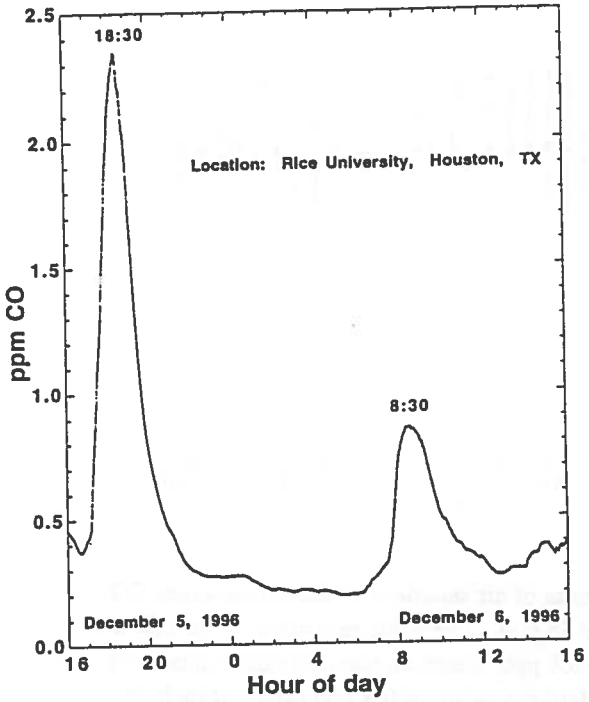

Fig. 6: CO concentration in room air versus time, recorded at Rice University on December 5th/6th, 1996. The multi-pass cell was left open to allow convective flow of air. The peaks were observed during the evening and morning rush house.

Line	Frequency (cm^{-1})	Isotope	Rotational Assignment	Vibrational Assignment
1	2154.46138	$^{15}N^{14}N^{16}O$	P(22)	$10^{1}0 - 10^{0}0$
2	2154.49222	$^{14}N^{14}N^{16}O$	P(54)	$11^{1}0 - 10^{1}/0$
3	2154.5644	$^{14}N^{15}N^{16}O$	P(11)	$11^{1}0 - 01^{1}/0$
4	2154.5839	$^{14}N^{15}N^{16}O$	P(11)	$11^{1}0 - 01^{1}e0$
5	2154.595583	$^{12}C^{16}O$	R(2)	1 – 0
6	2154.62121	$^{14}N^{14}N^{16}O$	P(54)	$11^{1}0 - 01^{1}e0$
7	2154.665±0.005	not identified		
8	2154.72236	$^{14}N^{15}N^{16}O$	P(25)	$10^{0}0 - 00^{0}0$
9	2154.740±0.005	not identified		
10	2154.8324	$^{14}N^{14}N^{16}O$	P(42)	$12^{0}0 - 02^{0}0$
11	2154.95091	$^{15}N^{14}N^{16}O$	P(21)	$02^{1}2 - 02^{0}2$
12	2154.87288	$^{14}N^{15}N^{16}O$	R(4)	$02^{1}2 - 02^{0f,e}2$

Table 1: List of infrared transitions identified in Figure 2. Transitions 7 and 9 could not be identified with the available literature.

Another source of stray absorption, particularly important in applications using diode lasers, is optical feedback. Free-running single-frequency Fabry-Perot lasers are particularly sensitive to optical feedback. Optical feedback from reflections and scattering into the diode laser can result in hysteresis and non-linearity of tuning, linewidth broadening and astounding amounts of excess intensity noise, mode hops, multi-mode operation, or even optical damage to the laser. Since the phase of optical feedback normally depends on vibration and temperature, both power and wavelength of the diode laser become unpredictable time-dependent functions of drive current, and that makes spectroscopy impossible. Even if back-reflections are eliminated by alignment, back-scattering may still degrade the tuning characteristics of a diode laser. To minimize the effect of optical feedback on the spectrum of the diode laser, the beam should be optically isolated right after it leaves the laser package. This does not guarantee complete removal of feedback, since it is almost impossible to avoid scattering in polarizers used with a given isolator, not to mention the collimating lens, usually present between the isolator and the diode chip.

Stray absorption can occur in air surrounding the beam path outside the sample volume, especially in *in situ* measurements. Ambient water vapor and carbon dioxide can routinely cause absorption of 10% and more over modest path lengths within a spectrometer.

There is another source of stray absorption which, in fact, has nothing to do with absorption. Diode-pumped DFG spectrometers operate with initial total probe power of a few microwatts CW, and only a fraction of this power is delivered to the signal detector. The signal detector is normally very quiet, with noise-equivalent power in the range of 1 - 100 pW · $Hz^{-1/2}$ corresponding to output voltage noise of 0.1 - 10 μV · $Hz^{-1/2}$. This *detector* noise may become a fundamental limitation to precision of the spectrometer. It is important that the detector noise be not exceeded by noise and interference introduced by signal processing. For example, a detector preamplifier adds intrinsic noise, and almost inevitably introduces amplified electromagnetic pickup from signals in other electronic devices.

5. SUMMARY

We described a portable solid-state mid-infrared spectrometer capable of fast measurements of carbon monoxide (CO) in air at atmospheric pressure. This instrument is based on quasi-phase-matched DFG in PPLN at room temperature, pumped by a 100 mW solitary diode laser at 865 nm and a 750 mW diode-pumped monolithic ring Nd:YAG laser at 1064.5 nm. The instrument produced 4.4 μW output power at 4.6 μm with less than 200 Mhz linewidth. Spectroscopic detection of CO was performed in air at atmospheric pressure and room temperature, flowing through a compact multipass cell with 18 m path length. For CO concentrations between 100 ppb and 9000 ppb, precision of 1 ppb was obtained for a signal averaging time of 20 s. Precision was limited by interference fringes from scattering in the multipass cell. The accuracy of the measurements was limited by the initial accuracy of the air sample used to calibration (0.5%).

This is the first demonstration of a portable, high-precision gas sensor based on diode-pumped mid-infrared DFG. The instrument employs no cryogenic or high-voltage components, measures 1 ft × 1 ft × 2 ft, and is controlled by a laptop computer. It showed reliable unattended operation in the field for more than 72 hours, without appreciable loss of output power or precision.

This technology has potential benefits for trace gas detection applications, since cost, power consumption, and size of the laser pump sources can be reduced further. For example, two fiber-coupled 10-100 mW diode lasers can be used as pump sources, one of the lasers being used in the external-cavity configuration for improved tuning range and predictability of wavelength. With bulk PPLN as the mixing element, reduction in pump power to 10 mW levels implies a factor of 750 reduction in DFG power, compromising the detection sensitivity. However, recently reported DFG conversion efficiencies for PPLN waveguide devices exceed $10\% \cdot W^{-1}$ [20], offering an excellent remedy for loss in pump power. Fiber coupling of the pump lasers into the waveguide would greatly improve stability of optical alignment, minimize sensitivity to vibration, significantly reduce size, and lower the cost of DFG sensor technology (Table 2).

Table 2: Characteristics of DFG Based CO Sensor

PARAMETER	CURRENT	PROJECTED
Wavelength	4.6 μm	3 – 5.3 and 8 – 12
Power	5 μW	100 μW (WG PPLN)
Linewidth	< 50 MHz	< 100 MHz
Detectors used	HgCdTe	InAs, HgCdTe
Environment	multipass cell, open air	open air
Detection limit	1 ppb	0.1 – 1 ppb
Dynamic range	0.1 – 100 ppm	0.1 – 100 ppm
Response time	1 – 60 s	1 – 10 s
Species detected	CO	NO, CO, N_2O, CO_2, SO_2, H_2CO, CH_4, H_2O
Pump power	50 mW + 500 mW	10 mW + 10 mW
Power supply	50 W	< 10 W
Lifetime	> 10,000 hrs	> 100,000 hrs
Size	2 cu.ft.	0.5 cu.ft.
Cost (prototype)	$80,000	$10,000

6. REFERENCES

1. A. Balakrishnan, S. Sanders, S. DeMars, J. Webjörn, D.W. Nam, R.J. Lang, D.G. Mehuys, R.F. Waarts, and D.F. Welch, "Broadly tunable laser-diode-based mid-infrared source with up to 31 μW of power at 4.3 μm wavelength," *Opt. Lett.* **21**, 952-954 (1996).

2. U. Simon, F.K. Tittel, and L. Goldberg, "Difference-frequency mixing in $AgGaS_2$ by use of a high-power GaAlAs tapered semiconductor amplifier at 860 nm," *Opt. Lett.* **18**, 1931-1933 (1993).

3. C.R. Webster, R.D. May, C.A. Trimble, R.G. Chave, and J. Kendall, "Aircraft (ER-2) laser infrared absorption spectrometer (ALIAS) for *in situ* stratospheric measurements of HCl, N_2O, CH_4, NO_2, and HNO_3," *Appl. Opt.* **33**, 454-472 (1994).

4. M. Zahniser, D.D. Nelson, J.B. McManus, and P.L. Kebabian, "Measurements of trace gas fluxes using tunable diode laser spectroscopy," *Phil. Trans. R. Soc. Lond. A* **351**, 371-382 (1995).

5. T.C. Hasenberg, R.H. Miles, A.R. Kost, and L. West, "Recent Advances in Sb-Based Midwave-Infrared Lasers," *IEEE J. Quantum Electron.* **33**, 1403-1406 (1997).

6. J. Faist, F. Capasso, C. Sirtori, D.L. Sivco, and A.L. Hutchinson, "High Power Mid-Infrared Quantum Cascade Lasers," *Appl. Phys. Lett.* **68**, 3680-3682 (1996).

7. L.E. Myers, G.D. Miller, R.C. Eckardt, M.M. Fejer, R.L. Byer, and W.R. Bosenberg, "Quasi-phase-matched 1.064-μm-pumped optical parametric oscillator in bulk periodically poled $LiNbO_3$," *Opt. Lett.* **20**, 52-54 (1995).

8. W.R. Bosenberg, A. Drobshoff, J.I. Alexander, L.E. Myers, and R.L. Byer, "93% pump depletion, 3.5-W continuous wave, singly resonant optical parametric oscillator," *Opt. Lett.* **21**, 336-1338 (1996).

9. K.P. Petrov, S. Waltman, E.J. Dlugokencky, M.A. Arbore, M.M. Fejer, F.K. Tittel, and L. Hollberg, "Precise measurement of methane in air using diode-pumped 3.4 μm difference-frequency generation in PPLN," *Appl. Phys. B* **64**, 567-572 (1997).

10. GEISA database, Laboratoire de Meteorologie Dynamique de C.N.R.S., Ecole Polytechnique 91128, Palaiseau Cedex, France.

11. A.G. Maki and J.S. Wells, *Wavenumber Calibration Tables from Heterodyne Frequency Measurements*, NIST Special Publication 821 (1991).

12. T. Töpfer, K.P. Petrov, Y. Mine, D. Jundt, R.F. Curl, and F.K. Tittel, "Room-temperature mid-infrared laser sensor for trace gas detection," *Appl. Opt.* **36**, 8042-8049 (1997).

13. T.-B. Chu and M. Broyer, "Intracavity CW difference-frequency generation by mixing three photons and using Gaussian laser beams," *J. de Phys.* **46**, 523-533 (1985).

14. L.E. Myers, Edward L. Ginzton Laboratory, Stanford, CA 94305, Ph.D. thesis, 1996.

15. W.H. Press, B.P. Flannery, S.A. Teukolsky, and W.T. Vetterling, *Numerical Recipes in Pascal*, Cambridge University Press, 572-580 (1989).

17. F.S. Pavone and M. Inguscio, "Frequency- and wavelength-modulation spectroscopies: comparison of experimental methods using an AlGaAs diode laser," *Appl. Phys. B* **56**, 118-122 (1993).

17. G. Guelachvili and K.N. Rao, *Handbook of Infrared Spectroscopy*, Academic Press 1986.

18. L.S. Rothman, R.R. Gamache, A. Goldman, L.R. Brown, R.A. Toth, H.M. Pickett, R.L. Poynter, J.-M. Flaud, C. Camy-Peyret, A. Barbe, N. Husson, C.P. Rinsland, and M.A.H. Smith, "The HITRAN database: 1986 edition," *Appl. Opt.* **26**, 4058-4097 (1987).

19. K.P. Petrov, R.F. Curl, and F.K. Tittel, "Compact laser-difference spectrometer for multi-component trace gas detection," accepted by *Applied Physics*, to appear in 1998.

20. M.A. Arbore, M.H. Chou, and M.M. Fejer, "Difference frequency mixing in $LiNbO_3$ waveguides using an adiabatically tapered periodically segmented coupling region," *CLEO Technical Digest Series 9*, 120 (1996).